Characterization of the [3Fe-4S] and [4Fe-4S] Clusters in Unbound PsaC Mutants C14D and C51D. Midpoint Potentials of the Single [4Fe-4S] Clusters Are Identical to F_A and F_B in Bound PsaC of Photosystem I†

Lian Yu,‡ Jindong Zhao,§ Weiping Lu,‡ Donald A. Bryant,§ and John H. Golbeck*,‡

Department of Biochemistry, Center for Biological Chemistry, University of Nebraska, Lincoln, Nebraska 68583-0718, and Department of Molecular and Cell Biology, Center for Biomolecular Structure and Function, The Pennsylvania State University, University Park, Pennsylvania 16802

Received February 16, 1993; Revised Manuscript Received April 30, 1993

ABSTRACT: In a previous paper we showed that the C51D mutant of PsaC contains a [3Fe-4S] cluster in the F_A site and a [4Fe-4S] cluster in the F_B site and that the C14D mutant contains an uncharacterized cluster in the F_B site and a [4Fe-4S] cluster in the F_A site [Zhao, J. D., Li, N., Warren, P. V., Golbeck, J. H., & Bryant, D. A. (1992) *Biochemistry 31*, 5093–5099]. In this paper we describe the electrochemical and electron spin resonance properties of the recombinant C14D and C51D holoproteins after *in vitro* reinsertion of the iron–sulfur clusters. Unbound PsaC shows no significant resonances in the oxidized state, but the unbound C14D and C51D mutant proteins show an intense set of resonances at $g \sim 2.02$ and 1.99 characteristic of an oxidized $[3Fe\text{-}4S]^{1+/0}$ cluster. The E_m' values for the $[3Fe\text{-}4S]^{1+/0}$ clusters in C14D (F_B*) and C51D (F_A*) are −98 mV, and both represent one-electron transfers. After reduction with dithionite at pH 10.0, wild-type PsaC shows a broad set of resonances resulting from the superposition of F_A^- and F_B^- characterized by a low-field peak at an apparent g value of 2.051 and a high-field trough at an apparent g value of 1.898. The F_B resonances in C51D were slightly narrower, with a low-field peak at an apparent g value of 2.039 and high-field trough at an apparent g value of 1.908. The F_A resonances in C14D were somewhat broader, with a low-field peak at an apparent g value of 2.042 and a high-field trough at an apparent g value of 1.898. The E_m' value for F_A in C14D is −515 mV, and the E_m' value for F_B in C51D is −580 mV; both represent one-electron transfers. These values are nearly identical to the E_m' values determined for the F_A and F_B clusters in PsaC bound to the photosystem I complex. This result indicates that the midpoint potentials of F_A and F_B are determined solely by the primary amino acid sequence of PsaC and not by interaction with PsaD or with the photosystem I core.

Photosystem I (PSI)[1] in green plants and cyanobacteria is an iron–sulfur, pigment–protein complex that transforms light into chemical free energy [reviewed in Almog et al. (1992), Sétif (1992), Bryant (1992), Golbeck (1992), and Ikeuchi (1992)]. The photosystem I core consists of a heterodimer of 82- and 83-kDa polypeptides, PsaA and PsaB, that includes ~100 antenna chlorophylls, a primary electron donor chlorophyll, a primary electron acceptor chlorophyll, two molecules of phylloquinone, and an interpolypeptide [4Fe-4S] cluster termed F_X. One quinone and the F_X cluster function as secondary electron acceptors to stabilize the charge separation between the primary donor and acceptor chlorophylls. A separate, but tightly bound, iron–sulfur protein, PsaC, functions as the tertiary electron acceptor, further stabilizing the charge separation and permitting soluble ferredoxin to be reduced with a high quantum efficiency. PsaC contains two [4Fe-4S] clusters, F_A and F_B, that pass electrons from F_X to ferredoxin.

PsaC is a low molecular mass polypeptide that contains 79 amino acids and two CxxCxxCxxxCP iron–sulfur binding motifs (Oh-oka et al., 1987). Although the three-dimensional structure has not been solved, there is enough primary sequence homology with the 54 amino acid *Peptococcus aerogenes* ferredoxin and the first 58 residues of the 106 amino acid *Azotobacter vinelandii* ferredoxin to predict a 2-fold rotation symmetry axis related to the two iron-sulfur binding sites (Dunn & Gray, 1988). The symmetry is imperfect, and the two iron-sulfur clusters have slightly different spectroscopic and redox properties. F_A is characterized by resonances at $g = 2.04$, 1.94, and 1.85, and F_B is characterized by resonances at $g = 2.07$, 1.92, and 1.89. When F_A and F_B are reduced in the same protein, the magnetic interaction between the two clusters leads to a merging of the high-field and low-field resonances, resulting in an interaction-type spectrum with resonances at $g = 2.05$, 1.94, 1.92, and 1.89 (Malkin & Bearden, 1971). The E_m' values of F_A and F_B have been measured to be −520 and −580 mV, respectively (Ke et al., 1973).

PsaC has been isolated and purified from higher plant and cyanobacterial thylakoids, but the resonances of the iron–sulfur clusters in the unbound protein are broad, making it impossible to distinguish F_A from F_B (Malkin et al., 1974). When PsaC is re-bound to the photosystem I core in the

† Published as Journal Series No. 10254 of the University of Nebraska Agricultural Research Division. Supported by grants from the National Science Foundation (MCB-9205756 to J.H.G. and MCB-9206851 to D.A.B.).

* Corresponding author.
‡ University of Nebraska.
§ The Pennsylvania State University.

[1] Abbreviations: Chl, chlorophyll; PSI, photosystem I; ESR, electron spin resonance; β-ME, β-mercaptoethanol; $NADP^+$, nicotinamide adenine dinucleotide phosphate; S/N, signal-to-noise ratio; F_A, [4Fe-4S] cluster ligated with cysteines 49, 51, 54, and 21; F_A*, [3Fe-4S] cluster ligated with cysteines 49, 54, and 21; F_B, [4Fe-4S] cluster ligated with cysteines 11, 14, 17, and 58; F_B*, [3Fe-4S] cluster ligated with cysteines 11, 17, and 58; EGTA, [ethylenebis(oxyethylenenitrilo]tetraacetic acid; IPTG, isopropyl-β-D-thiogalactopyranoside.

0006-2960/93/0432-8251$04.00/0

presence of PsaD, the resonances sharpen and appear identical to those of wild-type photosystem I complex (Mehari et al., 1991). The broad resonances preclude an accurate redox titration of the individual iron–sulfur clusters in unbound PsaC. By manipulating the experimental conditions, two redox species could be titrated in PsaC with approximate midpoint potentials of –470 and –560 mV (Oh-oka et al., 1991). The implication is that the former represents F_A and the latter F_B. Both potentials are more oxidizing than F_A and F_B in bound PsaC, but the increase in the midpoint potential of F_A is especially large and could indicate that a change in conformation of PsaC upon binding has a measurable effect on the thermodynamic properties of the iron-sulfur clusters.

Cyanobacterial *psaC* and *psaD* genes have been cloned and expressed in *Escherichia coli* (Zhao et al., 1990). Inclusion bodies containing the PsaC apoprotein can be solubilized in 7 M urea and refolded in buffer, and the iron–sulfur clusters can be reinserted with high efficiency using $FeCl_3$, Na_2S, and β-mercaptoethanol. When the PsaC holoprotein is re-bound to a P700-F_X core in the presence of PsaD, the F_A and F_B resonances sharpen to become identical to the control photosystem I complex (Li et al., 1991). Using site-directed mutagenesis coupled with this reconstitution protocol, we showed that the conversion of cysteine 51 to aspartic acid (C51D) results in a mutant protein containing one [3Fe-4S] cluster and one [4Fe-4S] cluster. We also showed that the conversion of cysteine 14 to aspartic acid (C14D) results in a mutant protein containing one uncharacterized cluster and one [4Fe-4S] cluster (Zhao et al., 1992). Because the photochemical behavior and spectroscopic properties of the [4Fe-4S] clusters in the C14D and C51D reconstituted photosystem I complexes were nearly identical to those of F_A and F_B in the wild-type photosystem I complex, we predicted that the redox potentials of the individual [4Fe-4S] clusters in the mutant proteins would be similar to their [4Fe-4S] counterparts in wild-type PsaC. In this paper, we measure the electrochemical properties of the $[3Fe\text{-}4S]^{1+/0}$ and $[4Fe\text{-}4S]^{2+/1+}$ clusters in the unbound C14D and C51D mutant proteins. We find that the [3Fe-4S] clusters in the F_A and F_B sites have relatively high midpoint potentials, while the [4Fe-4S] clusters in the unbound mutant C14D and C51D proteins have midpoint potentials nearly identical with those of F_A and F_B in photosystem I-bound PsaC.

MATERIALS AND METHODS

Plasmid Constructions and Expression of psaD and Mutant psaC Genes. The expression of the *psaD* gene of *Nostoc* sp. PCC 8009 in *E. coli* was described previously (Li et al., 1991). Construction of the mutant *psaC* genes was performed as described in Zhao et al. (1992) using appropriate synthetic oligonucleotides (24-mers) to prime second-strand synthesis. The construction of the C14D/C34S double mutant was performed using two mutagenic oligos (one for the D, one for the S) simultaneously in the extension reaction. The mutant *psaC* genes were recloned into plasmid pUC19 as *Xba*I–*Sst*I fragments and then subsequently recloned into the *Xba*I and *Nde*I sites of plasmid pET-3a (Studier et al., 1990). Overexpression of the mutant *psaC* genes was accomplished in *E. coli* strain BL21 (DE3), and cell disruption and inclusion body purification were performed as previously described (Zhao et al., 1990; Li et al., 1991).

Synthesis, Purification, and Reconstitution of the Mutant PsaC Proteins. E. coli strains harboring pET-36C (mutant *psaC*) and pET-3a/D (*psaD*) were grown in medium NYZCM (Sambrook et al., 1989) except that magnesium sulfate was omitted. The medium for cells synthesizing PsaC was supplemented with 50 μM ferric ammonium citrate (Zhao et al., 1990). Expression was performed essentially as described previously (Studier et al., 1990) and was initiated by the addition of IPTG to a final concentration of 0.5 mM to the growth medium. After 1 h, 20 μg/mL rifamycin was added to the medium, and expression was continued for an additional period of 5–7 h. Cells were harvested by centrifugation and washed once with TS buffer (20 mM Tris-HCl, pH 8.0, and 10 mM NaCl). Cells were resuspended in TS buffer containing 2 mM dithiothreitol and 2 μg/mL DNase and disrupted by two passes through a French pressure cell at 18 000 psi at 4 °C. Inclusion bodies were collected by centrifugation of the whole-cell extract at 7650*g* for 5 min at 4 °C. The inclusion bodies were resuspended in 25 mM Tris-HCl (pH 8.3) containing 2 mM dithiothreitol, and aliquots were overlayed on 15 mL of 10% (w/v) sucrose in Tris buffer. The inclusion bodies were collected by centrifugation at 14460*g* for 20 min at 4 °C and solubilized with 7 M urea, 2 mM DTT, and 2 mM EGTA in 50 mM Tris-HCl, pH 8.3. The solubilized proteins were purified by gel filtration over Sephadex G-75 and eluted with 2 mM DTT and 50 mM Tris-HCl, pH 8.3. Two protein bands were separated; the light brown band was collected for reconstitution. Protein concentration were determined using a dye-binding method (Bradford, 1976).

The iron–sulfur clusters were inserted into PsaC and the mutant proteins using a modification of the procotol of Parrett et al. (1989). The purified proteins were added to a final concentration of 0.5 mg/mL to a solution of 50 mM Tris-HCl (pH 8.3) containing 1% (v/v) β-mercaptoethanol. After 5 min of stirring at room temperature, a solution of 30 mM $FeCl_3$ was added slowly to a final concentration of 0.15 mM. After an additional 5 min of stirring, a solution of 30 mM Na_2S was added slowly to a final concentration of 0.15 mM. The reaction mixture was incubated at 4 °C for 12 h. The reconstituted iron–sulfur protein was purified free of inorganic reagents by repeated ultrafiltration over a YM-5 membrane (Amicon) and concentrated to a final protein concentration of 10–20 mg/mL.

Electron Spin Resonance Spectroscopy. Electron spin resonance (ESR) studies were performed with a Bruker ECS-106 X-band spectrometer. Cryogenic temperatures were maintained with an Oxford liquid helium cryostat and an Oxford ITC4 temperature controller. The microwave frequency was sampled during the run time with a Hewlett-Packard 5340A frequency counter. Sample temperatures were monitored by a calibrated thermocouple situated beneath the 3-mm-i.d. quartz sample tube and referenced to liquid nitrogen.

Electrochemical Redox Titrations. Samples of mutant proteins and redox dye solutions were depleted of oxygen by incubation at 4 °C in an anaerobic chamber for 12 h. The samples were placed in a laboratory-constructed electrochemical titration cell which was contiguous with an ESR sample tube (Harder et al., 1989). This design prevented the redox-poised sample from being exposed to oxygen during transfer to the ESR sample tube, which could alter the ambient potential and denature the iron–sulfur clusters. The electrochemical cell utilized a typical three-electrode circuit with Ag/AgCl reference and counter electrodes and a gold foil working electrode. A sample of dye solution was added to the cell to a final concentration of 0.5–1 mM. The cell was cycled several additional times with vacuum and argon purges. A potentiostat (CV-27, Bioanalytical Systems Inc., W. Lafayette, IN) was used to poise the potential at or slightly below the desired equilibrated potential. The potential of the system

was monitored by a high-impedance voltmeter across the working and reference electrodes after the potentiostat was turned off. When the potential no longer drifted, equilibrium was achieved. The cell was tipped to transfer the solution from the electrochemical pouch to the attached ESR sample tube. The tube was immersed in liquid nitrogen for analysis by ESR spectroscopy.

Data Analysis. The midpoint potential, E_m, was determined by fitting the titration data to the Nernst equation:

$$E = E_m + \frac{0.05}{n}\left[\log\left(\frac{[ox]}{[red]}\right)\right] \quad (1)$$

The intensity of the ESR lines is related to the microwave power according to Rupp et al. (1979)

$$S = A^* P^{0.5}/(1 + P/P_{1/2})^{0.5b} \quad (2)$$

where S is the signal intensity, A is a constant, P is the microwave power, $P_{1/2}$ is the power required to half-saturate the signal, and b is a constant (which varies from 1.0 for inhomogeneously broadened lines to 4.0 for homogeneously broadened lines). By fitting experimental data to eq 2, we found b to be almost equal to 1.0, and A and $P_{1/2}$ were different for the different iron–sulfur clusters.

Chemicals. Redox dyes used for the titration were as follows: 4,4′-dimethyl-*N*,*N*′-trimethylene-2,2′-dipyridinium dibromide, E_m = –680 mV; *N*,*N*′-trimethylene-2,2′-dipyridinium dibromide (TRIQUAT), E_m = –540 mV; methyl viologen, E_m = –440 mV; thionine, E_m = 56 mV; indigotetrasulfonic acid, E_m = –46 mV; indigodisulfonic acid, E_m = –125 mV. The first two dyes were synthesized as described by Salmon and Hawkridge (1980). All other dyes were purchased from Aldrich Chemical Co. and used without further purification.

RESULTS

ESR Spectra of [3Fe-4S]$^{1+/0}$ Clusters in C51D, C14D, and C14D/C34S Mutant Proteins. Figure 1 depicts the low-temperature ESR spectra of unbound C51D, C14D, and C14D/C34S mutant proteins under mildly oxidizing conditions. The holoproteins were fractionated from inorganic reconstitution agents by repeated ultrafiltration, but other than molecular oxygen, no oxidants or reductants were added. Wild-type PsaC, which contains 2[4Fe-4S]$^{2+/1+}$ clusters, is diamagnetic in the oxidized state and demonstrates no appreciable resonances in the g = 2 region (data not shown). The unbound C51D mutant has an intense axial spectrum in the oxidized state with a peak at g = 2.021 and a trough at g = 1.986 (Figure 1A). The presence of the $g \sim 2.02$ resonance, the line width of ~50 G, the general appearance of the signal, and the microwave power and temperature characteristics (see below) are all diagnostic of a [3Fe-4S]$^{1+/0}$ cluster (Moura et al., 1982; Münck, 1982; Beinert & Thomson, 1983). When C51D is re-bound to a P700-F_X core in the presence of PsaD, a reduced [4Fe-4S]$^{1+}$ cluster is found with g values characteristic of F_B; hence the [3Fe-4S] cluster is located in the F_A site (Zhao et al., 1992).

The unbound C14D mutant protein has a similar intense spectrum in the oxidized state with a peak at g = 2.019 and a trough at g = 1.987 (Figure 1B). The spectrum is nearly identical in appearance to that of C51D and differs only by a very slight narrowing of the low-field resonance. When C14D is re-bound to a P700-F_X core in the presence of PsaD, a reduced [4Fe-4S]$^{1+}$ cluster is found with g values characteristic of F_A; hence the [3Fe-4S] cluster is located in the F_B site (Zhao et al., 1992). The double mutant C14D/C34S was constructed to determine whether cysteine 34 has any role in conferring stability or function to the iron-sulfur clusters. This cysteine is conserved in 14 PsaC proteins from cyanobacteria and higher plants whose genes or proteins have been sequenced, but by analogy with soluble 2[4Fe-4S] ferredoxins, it is probably not a ligand to either F_A or F_B. The absence of the ninth cysteine at position 34 clearly has no deleterious effect on the ability of the F_B site to incorporate a [3Fe-4S] cluster (Figure 1C).

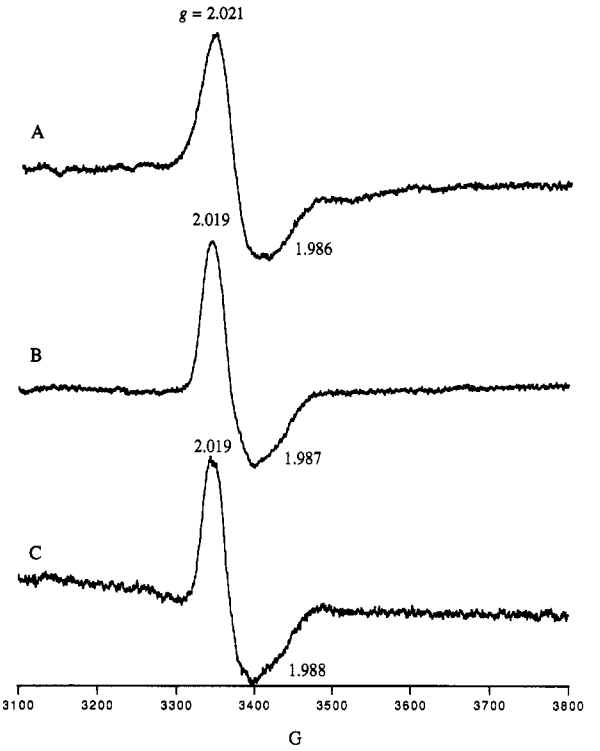

FIGURE 1: ESR spectra of mutant C51D (A), C14D (B) and C14D/C34S proteins (C) under mildly oxidizing conditions. The wild-type PsaC protein did not show any signals typical of [3Fe-4S] clusters. The g values of the low-field peak and the high-field trough are indicated. Spectrometer conditions: temperature, 30 K (C51D) and 60 K (C14D, C14D/C34S); microwave power, 5 mW; microwave frequency, 9.448 GHz; modulation amplitude, 10 G at 100 kHz.

ESR Spectra of [4Fe-4S]$^{2+/1+}$ Clusters in C51D, C14D, and C14D/C34S Mutant Proteins. Figure 2 depicts the low-temperature ESR spectra of wild-type PsaC and mutant proteins C51D, C14D, and C14D/C34S under strongly reducing conditions. Wild-type PsaC contains 2[4Fe-4S]$^{2+/1+}$ clusters which are paramagnetic in the reduced state. The spectrum of the unbound protein shows resonances in the g = 2 region (Figure 2A) with considerably broader line widths than PsaC bound to the photosystem I complex (Malkin et al., 1974). In spite of the broad spectrum, the shoulders at 3530 and 3560 G in the high-field region are consistent with the presence of two paramagnetic species. The midfield resonances of the F_A and F_B clusters are similarly merged, but the inflection at 3460 G also hints of two superimposed species. The low-field resonances are sufficiently weak to preclude meaningful analysis.

The reduced F_B cluster in the unbound C51D mutant protein is characterized by an axial-appearing spectrum (Figure 2B) with a low-field peak at an apparent g value of 2.039 and a high-field trough at an apparent g value of 1.908 (these are only empirical g values provided for the purpose of identification; the real g values can only be determined from simulations of the spectra). There is no indication of the presence of more than one paramagnetic species. When C51D is bound to the photosystem I core in the presence of PsaD,

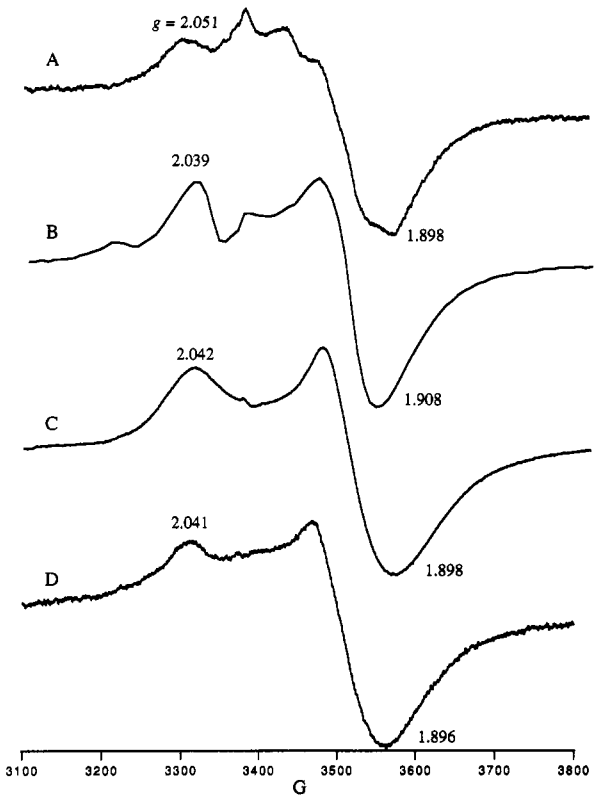

FIGURE 2: ESR spectra of wild-type PsaC (A) and mutant C51D (B), C14D (C), and C14D/C34S proteins (D) under strongly reducing conditions. PsaC and the mutant proteins from Figure 1 were exchanged by ultrafiltration into oxygen-free, 200 mM glycine, pH 10.0, and reduced with 1 mM sodium dithionite. The apparent g values of the principal resonances are determined empirically. Spectrometer conditions: temperature, 16 K; microwave power, 20 mW; microwave frequency, 9.448 GHz; modulation amplitude, 20 G at 100 kHz.

the peaks sharpen and the resulting rhobmic spectrum has resonances at $g = 2.043$, 1.942, and 1.853 (Zhao et al. 1992). The F_A cluster in the unbound C14D mutant protein shows a spectrum with resonances slightly broader than that of the F_B cluster in the C51D mutant protein (Figure 2C). A close comparison shows that the field position of the high-field resonance of F_A in C14D is higher than that of F_B in C51D, and the field position of the midfield resonance of F_A in C14D is slightly lower than that of F_B in C51D. However, the line widths and peak positions of F_A and F_B are sufficiently similar in the unbound mutant proteins to preclude identification of the clusters on the basis of g values alone. When C14D is bound to the photosystem I core in the presence of PsaD, the peaks sharpen and the resulting rhombic spectrum shows resonances at $g = 2.063$, 1.934, and 1.879 (Zhao et al. 1992). The double mutant C14D/C34S (Figure 2D) has the same spectral characteristics as C14D, indicating that the ninth cysteine at position 34 has no effect on the ability of the F_A site to incorporate a [4Fe-4S] cluster. This result and that shown in Figure 1C lead us to conclude that the function of the conserved cysteine 34 is unrelated to iron–sulfur binding.

Temperature Dependence of $[3Fe\text{-}4S]^{1+}$ *and* $[4Fe\text{-}4S]^{1+}$ *Clusters in C14D and C51D.* The electron spin relaxation properties of an iron–sulfur cluster can be studied by measuring the temperature dependence of the signals. Signal intensity, however, is a function of both temperature and microwave power and can be maximized only by adjusting both parameters. We optimized the F_A and F_B signals in PsaC and in the mutant C14D and C51D proteins with respect to S/N by measuring the signal intensity in a matrix of temperatures and powers. In general, the temperature/power profiles of the $[4Fe\text{-}4S]^{2+/1+}$ clusters in PsaC, C51D, C14D, and C14D/C34S were found to be similar, but not identical. In the analysis below, we chose the temperature and microwave power settings that provided the optimal S/N and then changed one of the parameters independently to compare the ESR characteristics of the various PsaC proteins.

Figure 3 shows the temperature dependence of the spectrum of reduced F_A and F_B in the unbound PsaC protein at 20 mW of microwave power. The intensity of the signals increases continuously as the temperature is lowered from 40 to 15 K and then begins to decrease in intensity from 12 to 8 K due to power saturation. At temperatures lower than 12 K, the signals are also accompanied by a slight change in line shape. The intensity of the peak at $g = 2.051$ and the trough at $g = 1.898$, plotted as a function of temperature, is maximum at 16 K (Figure 3, inset).

Figure 4A (open circles) depicts the effect of temperature on the intensity of the trough at $g = 1.908$ derived from the reduced [4Fe-4S] cluster (F_B) in C51D. At 40 K and 20 mW of microwave power, the F_B signal is broadened but still clearly visible, and it increases in intensity as the temperature is lowered, attaining a maximum at 16 K. At temperatures from 12 to 8 K the signal decreases in intensity, and it is accompanied by a change in line shape similar to that shown for F_A and F_B in unbound, wild-type PsaC (see Figure 3). Figure 4B (open squares) depicts the effect of temperature on the intensity of the trough at $g = 1.898$ derived from the reduced [4Fe-4S] cluster (F_A) in C14D. At 40 K and 20 mW of microwave power, the reduced F_A signal in C14D is broader and less intense than the F_B signal in C51D, but it increases rapidly in amplitude as the temperature is lowered, attaining a maximum at 16 K. This is consistent with a slightly faster electron spin relaxation for F_A than F_B, a finding in agreement with studies of F_A and F_B in bound PsaC (Rupp et al., 1979). At temperatures from 12 to 8 K, the signal decreases in intensity and is accompanied by a change in line shape similar to that found for F_B in C51D and for F_A/F_B in PsaC. The F_A cluster in the C14D/C51D protein had the same temperature characteristics as F_A in C14D.

Figure 4A (closed circles) depicts the effect of temperature on the intensity of the $g = 2.021$ resonance of the oxidized [3Fe-4S] cluster (F_A*) in C51D. At 5 mW of microwave power, the F_A* signal is barely visible at 80 K, and it increases in intensity as the temperature is lowered, attaining a maximum at 30 K. Figure 4B (closed squares) depicts the effect of temperature on the intensity of the $g = 2.019$ resonance of the oxidized [3Fe-4S] cluster (F_B*) in C14D. At 5 mW of microwave power, the F_B* signal is visible at temperatures approaching 100 K, and it shows a broader temperature range, attaining a maximum near 60 K. The F_B* cluster in the C14D/C51D double mutant had the same temperature characteristics as F_B* in C14D. These temperature profiles are within the range for known [3Fe-4S] clusters (Johnson et al., 1982).

Microwave Power Dependence of $[4Fe\text{-}4S]^{1+}$ *Clusters in C14D and C51D.* The relaxation properties of the F_A cluster in C14D and the F_B cluster in C51D were further studied by measuring the $P_{1/2}$ values for the reduced $[4Fe\text{-}4S]^{1+}$ clusters. A plot of log $(S/P^{0.5})$ against log P results in a straight line which is parallel to the abscissa when a signal is not saturated but which begins a downward deviation with the onset of power saturation. The intersection of the extrapolated lines gives the power for half-saturation (Rupp et al., 1978). In practice, $P_{1/2}$ is determined by curve-fitting the theoretical expression. Since the maximum signal amplitude for both F_A and F_B

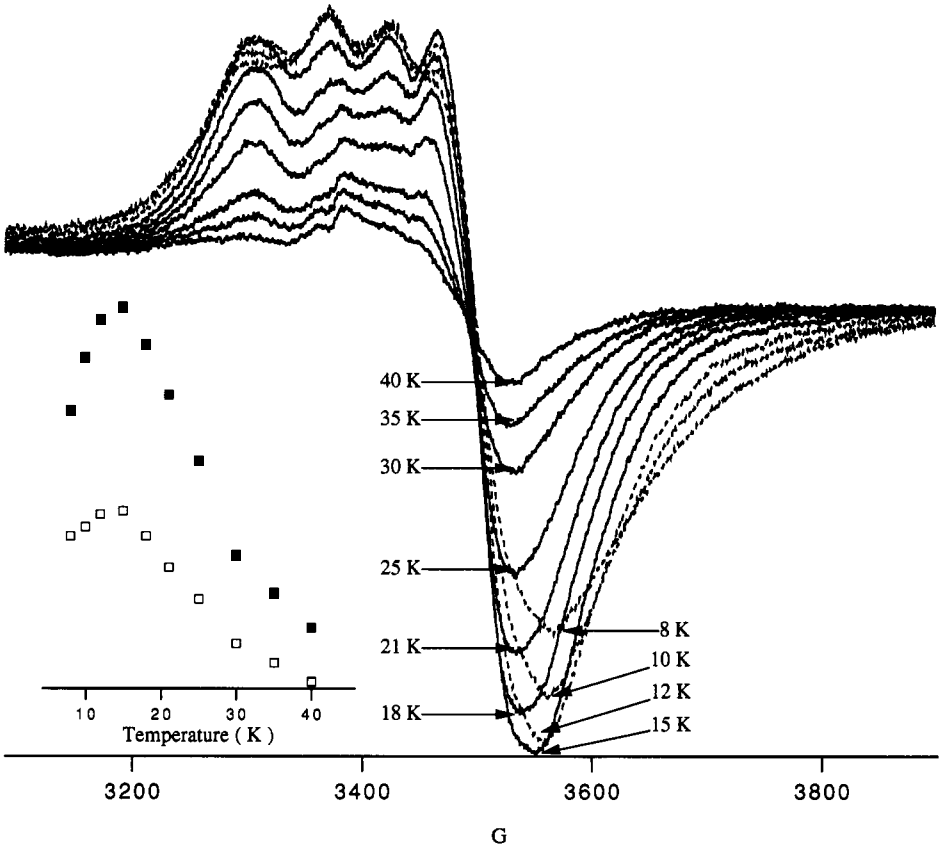

FIGURE 3: Temperature profiles of the reduced 2[4Fe-4S] clusters in unbound PsaC. The plotted spectra show the change in line shape with temperature at 20 mW of microwave power. The individual resonances of F_A and F_B cannot be separated. The composite high-field resonance at an apparent g value of 1.898 and the low-field resonance at an apparent g value of 2.051 are plotted against temperature in the inset.

occurs at a temperature of 16 K at a microwave power of 20–40 mW (this is actually the highest S/N; also, this value is instrument-dependent), the saturation studies were performed at this temperature. Figure 5 shows the effect of microwave power on the signal amplitude for the reduced $[4Fe\text{-}4S]^{1+}$ clusters in the C14D and C51D mutant proteins. The intersection of the horizontal and sloped lines for the $g = 1.898$ resonance of F_A indicates a $P_{1/2}$ of 50 mW for the [4Fe-4S] cluster in C14D. An analysis of F_B indicates a $P_{1/2}$ of 40 mW for the [4Fe-4S] cluster in C51D. The power saturation data is in line with the temperature data regarding the electron spin relaxation properties of F_A and F_B.

Redox Titrations of the $[3Fe\text{-}4S]^{1+/0}$ and $[4Fe\text{-}4S]^{2+/1+}$ Clusters in C14D and C51D. The results of an electrochemical redox titration of the $[3Fe\text{-}4S]^{1+/0}$ clusters in C51D, C14D, and C14D/C34S are shown in Figure 6. The midpoint potentials of the F_A* cluster in C51D (Figure 6A) and the F_B* cluster in C14D (Figure 6B, closed squares) and C14D/C34S (Figure 6B, open squares) were determined by plotting the intensity of the $g \sim 2.02$ resonances against the imposed potential. In all three titrations, the signal intensity decreased smoothly as the potential was raised from −150 to −60 mV. At potentials above −60 mV, the time required to attain redox equilibrium became prohibitive due to the oxidation of β-mercaptoethanol. The titrations also could not be performed in this region because all three proteins precipitate from solution in the absence of free thiol reagents. The data were analyzed by linearizing the Nernst equation and fitting the data according to a least-squares protocol. The E_m for the F_A* cluster in C51D was determined to be −98 mV; the E_m for the F_B* cluster in C14D was also −98 mV; and the E_m for the F_B* cluster in C14D/C34S was slightly lower, −92 mV. The same midpoint potential was obtained when the $g = 1.99$ trough was plotted against potential (data not shown). The number of electrons, n, involved in the electrochemical titration of the $[3Fe\text{-}4S]^{1+/0}$ cluster was 0.94 in C51D, 0.99 in C14D, and 1.00 in C14D/C34S (see eq 1 in Materials and Methods).

The results of an electrochemical redox titration of the $[4Fe\text{-}4S]^{2+/1+}$ clusters in C51D, C14D, and C14D/C34S are shown in Figure 7. The midpoint potentials of the F_B cluster in C51D (Figure 7A) and the F_A cluster in C14D (Figure 7B, closed squares) and C14D/C34S (Figure 7B, open squares) were determined by plotting the intensity of the high-field trough against the imposed potential. In all three mutants, the intensity of the resonant lines increased smoothly as the potential was lowered from −450 to −620 mV. The E_m for the F_B cluster in C51D was determined to be −580 mV; the E_m for the F_A cluster in C14D was −515 mV, and in C14D/C51D it was −523 mV. The number of electrons, n, involved in the electrochemical titration of the $[4Fe\text{-}4S]^{2+/1+}$ cluster was 1.09 in C51D, 0.98 in C14D, and 1.00 in C14D/C34S.

DISCUSSION

In an earlier publication (Li et al., 1991), we showed that the F_A and F_B iron–sulfur clusters could be reinserted into the PsaC protein concomitant with rebinding to the P700-F_X core. When the reconstitution was performed in the presence of PsaD, the resulting optical kinetics and ESR spectral characteristics of the charge separation between P700 and F_A/F_B were identical to those of a wild-type photosystem I complex. When the reconstitution was performed with the mutant protein C51D, the dark spectrum showed strong resonances with g values of 2.02 and 1.99 indicating a [3Fe-4S] cluster in the aspartate-containing site (Zhao et al., 1992). A set of resonances with g values of 2.063, 1.934, and 1.879 appeared

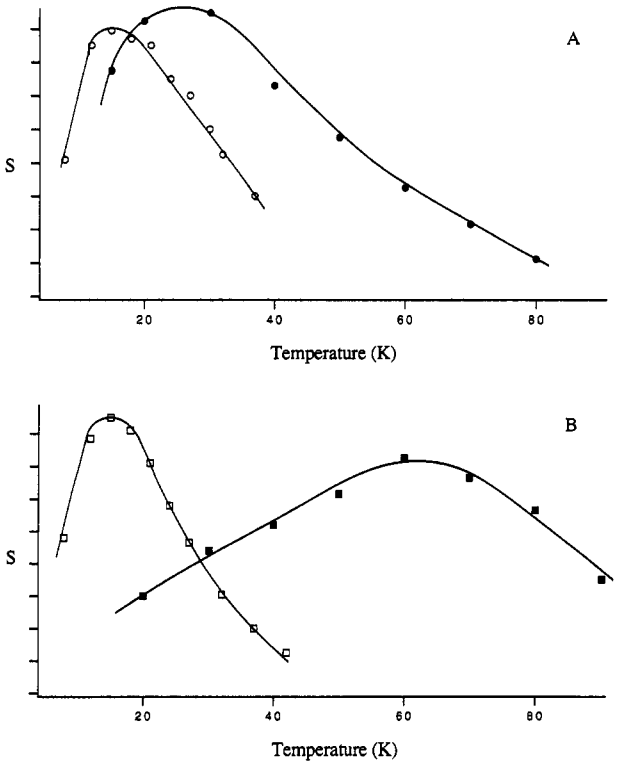

FIGURE 4: Temperature profiles of the iron–sulfur clusters in unbound C51D protein (A) and C14D protein (B). The [4Fe-4S] cluster data are shown as open symbols, and the [3Fe-4S] cluster data are shown as solid symbols. The intensity of the g = 2.02 peak was plotted against temperature in the case of the [3Fe-4S] clusters; the microwave power was 5 mW. The intensity of the high-field trough at an apparent g value of 1.908 was plotted versus temperature for the [4Fe-4S] cluster in C51D, and the high-field trough at an apparent g value of 1.898 was plotted versus temperature for the [4Fe-4S] cluster in C14D; the microwave power was 20 mW.

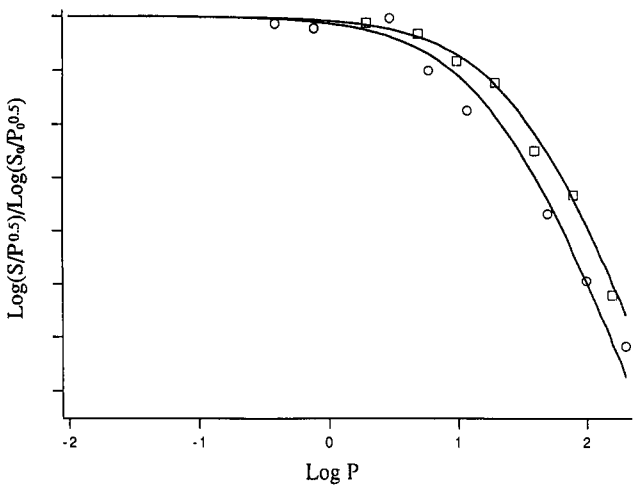

FIGURE 5: Microwave power studies of the [4Fe-4S] clusters in unbound mutant C51D and C14D proteins. The C14D protein data are depicted as squares, and the C51D protein data are depicted as circles. The intensity of the high-field trough at an apparent g value of 1.908 was plotted versus microwave power for the [4Fe-4S] cluster in C51D, and the intensity of the high-field trough at an apparent g value of 1.898 was plotted versus microwave power for the [4Fe-4S] cluster in C14D; the temperature was 16 K.

in the light which identified the [4Fe-4S] cluster as F_B. When the reconstitution was performed with mutant protein C14D, the dark spectrum showed strong resonances with an usual set of g values that left uncertain the identification of the cluster in the aspartate-containing site (Zhao et al., 1992). A set of resonances with g values of 2.043, 1.942, and 1.853 appeared

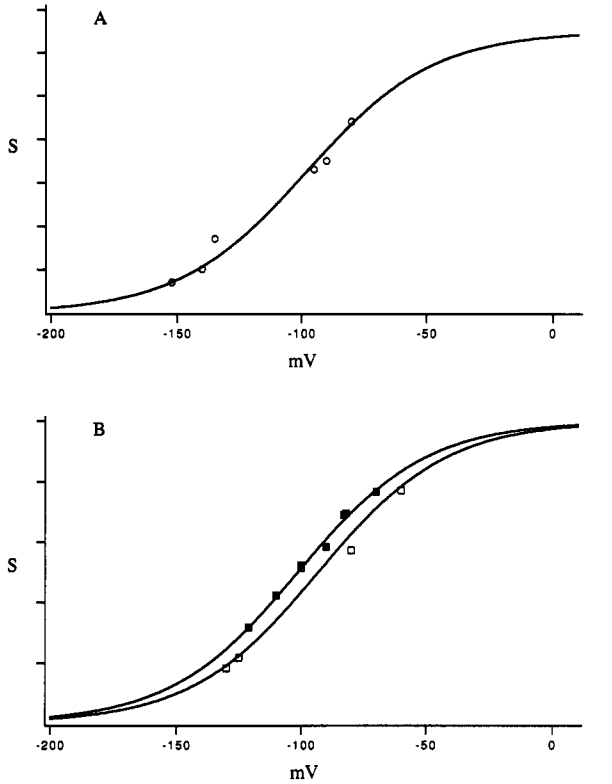

FIGURE 6: Redox titration of the $[3Fe\text{-}4S]^{1+/0}$ clusters in unbound C51D (A), C14D (B, closed squares), and C14D/C34S (B, open squares) after reconsitution of the iron–sulfur clusters. Symbols represent experimental data; the solid line is a theoretical fit to the Nernst equation. The n and E_m values are calculated as described in Materials and Methods.

in the light which identified the [4Fe-4S] cluster as F_A. Because only 12% of the F_B cluster was photoreduced in the C51D mutant, whereas about 73% of the F_A cluster was photoreduced in the C14D mutant, we suggested that F_B was not an obligatory intermediate in the low-temperature pathway of electrons to F_A. The tacit assumption was that the [3Fe-4S] cluster had a midpoint potential higher than the [4Fe-4S] clusters it had replaced, rendering it incapable of forward electron flow.

We tested that assumption in the present work. First, we showed that it was possible to insert a [3Fe-4S] cluster as well as a [4Fe-4S] cluster into the recombinant C14D and C51D apoproteins using $FeCl_3$, Na_2S, and β-mercaptoethanol. This indicates that the unbound C14D mutant protein (as well as the unbound C51D mutant protein) is able to support a [3Fe-4S] cluster in the aspartate-containing site. Given that the naturally occurring [3Fe-4S] ferredoxin from *Pyrococcus furiosus* (Connover et al., 1991; Park et al., 1991) and [3Fe-4S] [4Fe-4S] ferredoxin from *Desulfovibrio africanus* (George et al., 1989; Armstrong et al., 1989) also contain an aspartic acid in a similar position, the existence of a [3Fe-4S] cluster may be a predictable response to this amino acid change. Whether a [3Fe-4S] cluster can exist when other cysteines in the CxxCxxCxxxCP iron–sulfur binding motif are changed to aspartate remains to be determined. Second, the appearance of the ESR resonances from the reduced $[4Fe\text{-}4S]^{1+}$ clusters in unbound PsaC, C14D, or C15D is very different from those when the proteins are bound to the photosystem I complex. In particular, the spectra of unbound PsaC, C14D, and C51D show significantly broader line widths relative to the bound protein [see Mehari et al. (1990)]. In fact, the C14D and C51D proteins resemble the soluble [3Fe-4S] [4Fe-4S] ferredoxin II isolated from *Rhodobacterium capsulatum*

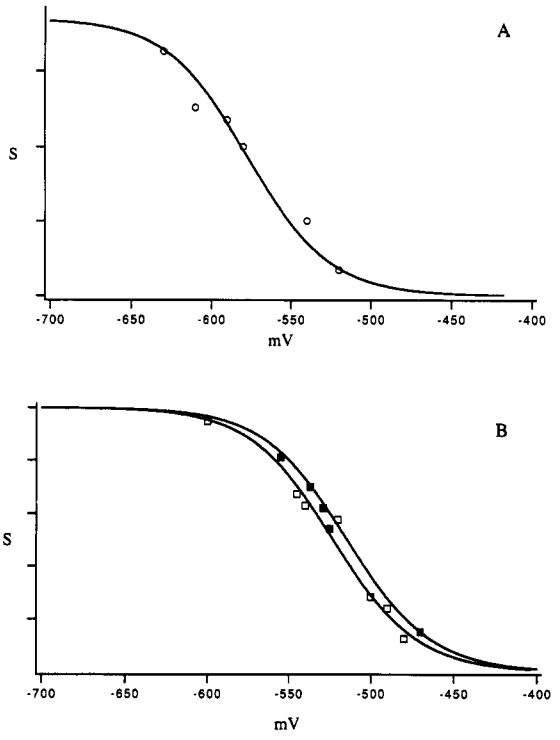

FIGURE 7: Redox titration of the $[4Fe\text{-}4S]^{2+/1+}$ clusters in unbound C51D (A), C14D (B, closed squares), and C14D/C34S (B, open squares) after reconstitution of the iron–sulfur clusters. The microwave power was 10 mW; the temperature for C51D and C14D was 16 K. Symbols represent experimental data; the solid line is a theoretical fit to the Nernst equation. The n and E_m values are calculated as described in Materials and Methods.

(Jouanneau et al., 1990). The spectral features of PsaC, C14D, and C51D are fully reversible in that the narrow line widths are restored when the proteins are re-bound to the P700-F_X core in the presence of PsaD (data not shown). Third, the midpoint potentials of the [3Fe-4S] clusters in both C14D and C51D have been found to be a relatively high –98 mV. This value is within the midrange for [3Fe-4S] clusters in aconitase (0 mV) [see Beinert and Thomson (1983)], in ferredoxin II from *Desulfovibrio gigas* (–130 mV) [Huynh et al., 1980], and from oxidatively denatured ferredoxin from *Bacillus stearothermophilus* (0 mV) [see Beinert and Thomson, 1983)], but is is considerably less reducing than the [3Fe-4S] cluster in ferredoxins isolated from *Thermus thermophilus* (–230 mV) (Ohnishi et al. 1980; Hille et al., 1983), *Streptomyces griseus* (<–400 mV) (Trower et al., 1990), *Azotobacter vinelandii* (–420 mV) (Emptage et al., 1980), and *Azotobacter chroococcum* (–460 mV) (Armstrong et al., 1988). It is particularly interesting that the midpoint potential is close to that determined for the [3Fe-4S] cluster in the *D. afracinus* ferredoxin III (–90 mV) (George et al., 1989), in which an aspartic acid similarly replaces the second cysteine in the CxxCxxCxxxCP iron–sulfur binding motif.

Due to the broad line widths, it was not possible to determine whether the F_A or the F_B iron–sulfur cluster was present in the unbound C14D and C51D proteins on the basis of g values alone. However, we had previously identified F_A as the [4Fe-4S] cluster in C14D and F_B as the [4Fe-4S] cluster in C51D from the g values of the sharp resonances after rebinding the mutant proteins to a P700-F_X core in the presence of PsaD (Zhao et al., 1992). In the present study, the midpoint potential of the [4Fe-4S] cluster in C14D was determined to be –515 mV, and that of the [4Fe-4S] cluster in C51D was determined to be –580 mV; both represent one-electron transfers. These midpoint potentials are nearly identical to those of F_A (–520 mV) and F_B (–580 mV) in bound PsaC in cyanobacterial and spinach photosystem I (Ke et al., 1973, Heathcote et al., 1978). These results, along with the spin relaxation properties of [4Fe-4S] clusters in the mutant proteins, are consistent with our original conclusion that F_A is ligated by cysteines 49, 51, 54, and 21 and that F_B is ligated by cysteines 11, 14, 17, and 58 in the PsaC protein of photosystem I (Zhao et al., 1992). These results show that the primary amino acid sequence of PsaC, and not the interaction of PsaC with PsaD or with the photosystem I core, is the primary determinant of the redox potentials of the iron–sulfur clusters. It also indicates that the presence of a [3Fe-4S] cluster does not influence the redox potential of the [4Fe-4S] cluster in either mutant protein. Since the properties of F_B could only be determined previously in the presence of reduced F_A, the result with the mutant C51D protein further shows that the midpoint potential of F_B is not affected by F_A^- and must be an inherent property of the cluster.

Two groups have reported the oxidation–reduction properties of the iron–sulfur clusters in unbound spinach PsaC as determined by redox potentiometry and ESR spectroscopy. Although the broad resonances in PsaC precluded titration of the individual clusters at 10 K, Oh-oka and colleagues (1991) took advantage of the rapid spin relaxation characteristics of one of the clusters to "isolate" one of the two redox centers. The redox behavior of the species that remained visible at 38 K, cluster 1, was consistent with a one-electron titration and an approximate E_m value of –470 mV. The redox titration at 10 K covered a broader span than at 38 K, a finding consistent with the presence of two redox components. When fitted to a one-electron reduction, the E_m value of cluster 2 was found to be around –560 mV. On the basis of the relative potentials, it was suggested that $E_{m,1}$ corresponds to F_A and $E_{m,2}$ corresponds to F_B. However, the lack of data points at 38 K in the 120-mV span which encompasses 10–90% reduction of the cluster [closed circles in Figure 5 of Oh-oka et al. (1991)] makes it very difficult to assign the E_m value of –470 mV to F_A with a high degree of confidence. Given this uncertainity, we are reluctant to claim a discrepancy with the E_m value of –515 mV determined for F_A in this study for the unbound C14D mutant. Due to a higher S/N and a larger number of relevant data points in the relevant 120-mV span, the quality of the 10 K titration data [open circles in Figure 5 of Oh-oka et al. (1991)] is much better. The reported $E_{m,2}$ value of –560 mV is closer to the E_m value of –580 mV determined for F_B in the unbound C51D mutant. In contrast, Hanley and colleagues (1992) reported a single wave in the titration of spinach PsaC with an E_m of –510 mV, with no evidence for different potentials in the two centers. However, there conditions differed from those of Oh-oka, in that 25% glycerol was included in the medium to stabilize the iron–sulfur clusters. Since it is known that F_A and F_B in a photosystem I complex shift about 30 and 45 mV more positive in 50% glycerol (Evans & Heathcote, 1980), a similar effect could have influenced the E_m' of the iron–sulfur clusters in the unbound PsaC protein. This, however, remains to be tested. We suggest that the midpoint potentials of F_A and F_B in the unbound PsaC protein from spinach are most likely identical to that of F_A in the C14D mutant and F_B in the C51D mutant proteins derived from *Synechococcus* sp. PCC 7002 PsaC. These results indicate that the relatively low E_m values for the F_A and F_B clusters are a function of the structure of the PsaC protein, and are not a result of the interaction of PsaC with PsaD or with the photosystem I core.

REFERENCES

Almog, O., Shoham, G. & Nechushtai, R. (1992) in *The Photosystems: Structure, Function, and Molecular Biology* (Barber, J., Ed.) pp 443–469, Elsevier, Amsterdam.

Armstrong, F. A., George, S. J., Cammack, R., Hatchikian, E. C., & Thomson, A. J. (1989) *Biochem. J. 264*, 265–273.

Beinert, H., & Thomson, A. J. (1983) *Arch Biochem. Biophys. 222*, 333–361.

Bradford, M. M. (1976) *Anal. Biochem. 72*, 248–254.

Bryant, D. (1992) In *The Photosystems: Structure, Function, and Molecular Biology* (Barber, J., Ed.) pp 501–549, Elsevier, Amsterdam.

Dunn, P. P. J., & Gray, J. C. (1988) *Plant Mol. Biol. 11*, 311–319.

Emptage, M. H., Kent, T. A., Huynh, B. H., Rawlings, J., Orme-Johnson, W. H., & Münck, E. (1980) *J. Biol. Chem. 255*, 1793–1796.

Evans, M. C. W., & Heathcote, P. (1980) *Biochim. Biophys. Acta 590*, 89–96.

George, S. J., Armstrong, F. A., Hatchikian, E. C., & Thomson, A. J. (1989) *Biochem. J. 264*, 275–284.

Golbeck, J. H. (1992) *Annu. Rev. Plant Physiol. Plant Mol. Biol. 43*, 293–324.

Hanley, J. A., Kear, J., Bredenkamp, G., Li, G., Heathcote, P., & Evans, M. C. W. (1992) *Biochim. Biophys. Acta 1099*, 152–156.

Harder, S. R., Lu, W. P., Feinberg, B. A., & Ragsdale, S. W. (1989) *Biochemistry 28*, 9080–9087.

Heathcote, P., Williams-Smith, D. L., Sihra, C. K., & Evans, M. C. W. (1978) *Biochim. Biophys. Acta 503*, 333–342.

Hille, R., Yoshida, T., Tarr, G. E., Williams, C. H., Jr., Ludwig, M. L., Fee, J. A., Kent, T. A., Huynh, B. H., & Münck, E (1983) *J. Biol. Chem. 258*, 13008–13013.

Huynh, B. H., Boura, J. G., Moura, I., Kent, T. A., Legall, J., Xavier, A. V., & Münck, E. (1980) *J. Biol. Chem. 255*, 3242–3244.

Ikeuchi, M. (1992) *Plant Cell Physiol. 33*, 669–676.

Johnson, M. K., Spiro, T. G., & Mortenson, L. E. (1982) *J. Biol. Chem. 257*, 2447–2452.

Jouanneau, Y., Meyer, C., Gaillard, J., & Vignais, P. M. (1990) *Biochem. Biophys. Res. Commun. 171*, 273–279.

Ke, B., Hansen, R. E., & Beinert, H. (1973) *Proc. Natl. Acad. Sci. U.S.A. 70*, 2941–2945.

Li, N., Zhao, J. D., Warren, P. V., Warden, J. T., Bryant, D. A., & Golbeck, J. H. (1991) *Biochemistry 30*, 7853–7872.

Malkin, R., & Bearden, A. J. (1971) *Proc. Natl. Acad. Sci. U.S.A. 68*, 16–19.

Malkin, R., Aparicio, P. J., & Arnon, D. I. (1974) *Proc. Natl. Acad. Sci. U.S.A. 71*, 2362–2366.

Mehari, T., Parrett, K. G., Warren, P. V., & Golbeck, J. H. (1991) *Biochim. Biophys. Acta 1056*, 139–148.

Moura, J. J. G., Moura, I., Kent, T. A., Lipscomb, J. D., Huynh, B. H., LeGall, J., Xavier, A. V., & Münck, E. (1982) *J. Biol. Chem. 257*, 6259–6267.

Münck, E. (1982) in *Iron–Sulfur Proteins* (Spiro, T. G., Ed). Chapter 4, Academic Press, New York.

Ohnishi, T., Blum, H., Sato, S., Nahazawa, K., Hon-nami, K., & Oshima, T. (1980) *J. Biol. Chem. 255*, 345–348.

Oh-Oka, H., Takahashi, Y., Wada, K., Matsubara, H., Ohyama, K., & Ozeki, H. (1987) *FEBS Lett. 218*, 52–54.

Oh-oka, H., Itoh, S., Saeki, K., Takahashi, Y., & Matsubara, H. (1991) *Plant Cell Physiol. 32*, 11–17.

Park, J. B., Fan, C. L., Hoffman, B. M., & Adams, M. W. W. (1991) *J. Biol. Chem. 266*, 19351–19356.

Parrett, K. G., Mehari, T., Warren, P. V., & Golbeck, J. H. (1989) *Biochim. Biophys. Acta 973*, 324–332.

Rupp, H., Rao, K. K., Hall, D. O., & Cammack, R. (1978) *Biochim. Biophys. Acta 537*, 255–269.

Rupp, H., De la Torre, A., & Hall, D. O. (1979) *Biochim. Biophys. Acta 548*, 552–564.

Salmon, R. T., & Hawkridge, F. M. (1980) *J. Electroanal. Chem. Interfacial Electrochem. 112*, 253–264.

Sambrook, J., Fritsch, E. F., & Maniatis, T. (1989) *Molecular Cloning: A Laboratory Manual*, 2nd ed., Cold Spring Harbor Laboratory Press, Cold Spring Harbor, New York.

Sétif, P. (1992) in *The Photosystems: Structure, Function, and Molecular Biology* (Barber, J., Ed.) pp 471–499, Elsevier, Amsterdam.

Studier, F. W., Rosenberg, A. H., Dunn, J. J., & Dubendorff, J. W. (1990) *Methods Enzymol. 185*, 60–88.

Trower, M. K., Emptage, M. H., & Sariaslani, F. S. (1990) *Biochim. Biophys. Acta 1037*, 281–289.

Zhao, J. D., Warren, P. V., Li, N., Bryant, D. A., & Golbeck, J. H. (1990) *FEBS Lett. 276*, 175–180.

Zhao, J. D., Li, N., Warren, P. V., Golbeck, J. H., & Bryant, D. A. (1992) *Biochemistry 31*, 5093–5099.